

Effective indicators for diagnosis of oral cancer using optical coherence tomography

Meng-Tsan Tsai,¹ Hsiang-Chieh Lee,¹ Cheng-Kuang Lee,¹ Chuan-Hang Yu,² Hsin-Ming Chen,² Chun-Pin Chiang,² Cheng-Chang Chang,¹ Yih-Ming Wang,¹ and C. C. Yang^{1,3*}

¹Institute of Photonics and Optoelectronics, National Taiwan University, 1, Roosevelt Road, Section 4, Taipei, Taiwan

²Department of Dentistry, National Taiwan University, Taipei, Taiwan

³Department of Electrical Engineering, National Taiwan University, Taipei, Taiwan

*corresponding author: ccy@cc.ee.ntu.edu.tw

Abstract: A swept-source optical coherence tomography system is used to clinically scan oral precancer and cancer patients for statistically analyzing the effective indicators of diagnosis. Three indicators are considered, including the standard deviation (SD) of an A-mode scan signal profile, the exponential decay constant (α) of an A-mode-scan spatial-frequency spectrum, and the epithelium thickness (T) when the boundary between epithelium and lamina propria can still be identified. Generally, in abnormal mucosa, the standard deviation becomes larger, the decay constant of the spatial-frequency spectrum becomes smaller, and epithelium becomes thicker. The sensitivity and specificity of the three indicators are discussed based on universal and individual relative criteria. It is found that SD and α are good diagnosis indicators for moderate dysplasia and squamous cell carcinoma. On the other hand, T is a good diagnosis indicator for epithelia hyperplasia and moderate dysplasia.

©2008 Optical Society of America

OCIS codes: (110.4500) Optical Coherence Tomography; (170.3880) Medical and biological imaging

References and links

1. M. Lingen, E. M. Sturgis, and M. S. Kies, "Squamous cell carcinoma of the head and neck in non-smokers: clinical and biologic characteristics and implications for management," *Curr. Opin. Oncol.* **13**, 176-182 (2001).
2. D. M. Parkin, F. Bray, J. Ferlay, and P. Pisani, "Global cancer statistics, 2002," *CA Cancer J. Clin.* **55**, 74-108 (2005).
3. A. Jemal, T. Murray, E. Ward, A. Samuels, R. C. Tiwari, A. Ghafoor, E. J. Feuer, and M. J. Thun, "Cancer statistics, 2005," *CA Cancer J. Clin.* **55**, 10-30 (2005).
4. B. W. Neville, D. D. Damm, C. M. Allen, and J. E. Bouquot, *Oral and maxillofacial pathology*, 2nd ed., (2002), pp. 337-346.
5. D. Huang, E. A. Swanson, C. P. Lin, J. S. Schuman, W. G. Stinson, W. Chang, M. R. Hee, T. Flotte, K. Gregory, C. A. Puliafito, and J. G. Fujimoto, "Optical Coherence Tomography," *Science* **254**, 1178-1181 (1991).
6. D. C. Adler, Y. Chen, R. Huber, J. Schmitt, J. Connolly, and J. G. Fujimoto, "Three-dimensional endomicroscopy using optical coherence tomography," *Nature Photon.* **1**, 709-716 (2007).
7. A. F. Fercher, C. K. Hitzenberger, G. Kamp, and S. Y. Elzaiat, "Measurement of Intraocular Distances by Backscattering Spectral Interferometry," *Opt. Commun.* **117**, 43-48 (1995).
8. S. Yun, G. Tearney, B. Bouma, B. Park, and J. de Boer, "High-speed spectral-domain optical coherence tomography at 1.3 μm wavelength," *Opt. Express* **11**, 3598-3604 (2003), <http://www.opticsexpress.org/abstract.cfm?uri=oe-11-26-3598>.
9. M. Wojtkowski, V. Srinivasan, T. Ko, J. Fujimoto, A. Kowalczyk, and J. Duker, "Ultrahigh-resolution, high-speed, Fourier domain optical coherence tomography and methods for dispersion compensation," *Opt. Express* **12**, 2404-2422 (2004), <http://www.opticsexpress.org/abstract.cfm?uri=oe-12-11-2404>.
10. B. Cense, N. Nassif, T. Chen, M. Pierce, S. H. Yun, B. Park, B. Bouma, G. Tearney, and J. de Boer, "Ultrahigh-resolution high-speed retinal imaging using spectral-domain optical coherence tomography," *Opt. Express* **12**, 2435-2447 (2004), <http://www.opticsexpress.org/abstract.cfm?URI=OPEX-12-11-2435>.
11. S. H. Yun, G. J. Tearney, J. F. de Boer, N. Ifimia, and B. E. Bouma, "High-speed optical frequency-domain imaging," *Opt. Express* **11**, 2953-2963 (2003), <http://www.opticsexpress.org/abstract.cfm?id=77825>.

12. R. Huber, D. C. Adler, and J. G. Fujimoto, "Buffered Fourier domain mode locking: unidirectional swept laser sources for optical coherence tomography imaging at 370,000 lines/s," *Opt. Lett.* **31**, 2975-2977 (2006).
13. J. F. de Boer, B. Cense, B. H. Park, M. C. Pierce, G. J. Tearney, and B. E. Bouma, "Improved signal-to-noise ratio in spectral-domain compared with time-domain optical coherence tomography," *Opt. Lett.* **28**, 2067-2069 (2003).
14. R. Leitgeb, C. K. Hitzenberger, and A. F. Fercher, "Performance of Fourier domain vs. time domain optical coherence tomography," *Opt. Express* **11**, 889-894(2003), <http://www.opticsexpress.org/abstract.cfm?URI=OPEX-11-8-889>.
15. M. A. Choma, M. V. Sarunic, C. H. Yang, and J. A. Izatt, "Sensitivity advantage of swept source and Fourier domain optical coherence tomography," *Opt. Express* **11**, 2183-2189 (2003), <http://www.opticsexpress.org/abstract.cfm?uri=OE-11-18-2183>.
16. J. Zhang, Q. Wang, B. Rao, Z. Chen, and K. Hsu, "Swept laser source at 1 μm for Fourier domain optical coherence tomography," *Appl. Phys. Lett.* **89**, 073901 (2006).
17. Y. Yasuno, Y. Hong, S. Makita, M. Yamanari, M. Akiba, M. Miura, and T. Yatagai, "*In vivo* high-contrast imaging of deep posterior eye by 1- μm swept source optical coherence tomography and scattering optical coherence angiography," *Opt. Express* **15**, 6121-6139 (2007), <http://www.opticsexpress.org/abstract.cfm?uri=oe-15-10-6121>.
18. B. W. Colston, Jr., M. J. Everett, L. B. Da Silva, L. L. Otis, P. Stroeve, and H. Nathel, "Imaging of hard and soft-tissue structure in the oral cavity by optical coherence tomography," *Appl. Opt.* **37**, 3582-3585 (1998).
19. B. W. Colston, Jr., M. J. Everett, U. S. Sathyam, L. B. DaSilva, and L. L. Otis, "Imaging of the oral cavity using optical coherence tomography," *Monogr. Oral Sci.* **17**, 32-55 Review (2000).
20. L. L. Otis, M. J. Everett, U. S. Sathyam, B. W. Colston, Jr., "Optical coherence tomography: a new imaging technology for dentistry," *J. Am. Dent. Assoc.* **131**, 511-514 (2000).
21. E. Matheny, N. Hanna, W. Jung, Z. Chen, and P. Wilder-Smith, "Optical coherence tomography of malignancy in hamster cheek pouches," *J. Biomed. Opt.* **9**, 978-981 (2004).
22. P. Wilder-Smith, W. G. Jung, M. Brenner, K. Osann, H. Beydoun, D. Messadi, and Z. Chen, "In vivo optical coherence tomography for the diagnosis of oral malignancy," *Lasers Surg. Med.* **35**, 269-275 (2004).
23. A. L. Clark, A. Gillenwater, R. Alizadeh-Naderi, A. K. El-Naggar, and R. Richards-Kortum, "Detection and diagnosis of oral neoplasia with an optical coherence microscope," *J. Biomed. Opt.* **9**, 1271-1280 (2004).
24. W. Jung, J. Zhang, J. Chung, P. Wilder-Smith, M. Brenner, J. S. Nelson, and Z. Chen, "Advances in Oral Cancer Detection using Optical Coherence Tomography," *IEEE J. Select. Topics Quantum Electron.* **11**, 811-817 (2005).
25. N. M. Hanna, W. Waite, K. Taylor, W. G. Jung, D. Mukai, E. Matheny, K. Kreuter, P. Wilder-Smith, M. Brenner, and Z. Chen, "Feasibility of three-dimensional optical coherence tomography and optical Doppler tomography of malignancy in hamster cheek pouches," *Photomed. Laser Surg.* **24**, 402-409 (2006).
26. J. M. Ridgway, W. B. Armstrong, S. Guo, U. Mahmood, J. Su, R. P. Jackson, T. Shibuya, R. L. Crumley, M. Gu, Z. Chen, and B. J. Wong, "In vivo optical coherence tomography of the human oral cavity and oropharynx," *Arch. Otolaryngol. Head Neck Surg.* **132**, 1074-1081 (2006).
27. B. Wong, R. Jackson, S. Guo, J. Ridgway, U. Mahmood, J. Shu, T. Shibuya, R. Crumley, M. Gu, W. Armstrong, and Z. Chen, "In Vivo Optical Coherence Tomography of the Human Larynx: Normative and Benign Pathology in 82 Patients," *The Laryngoscope* **115**, 1904-1911 (2005).
28. W. Armstrong, J. Ridgway, D. Vokes, S. Guo, J. Perez, R. Jackson, M. Gu, J. Su, R. Crumley, T. Shibuya, U. Mahmood, Z. Chen, and B. Wong, "Optical Coherence Tomography of Laryngeal Cancer," *The Laryngoscope* **116**, 1107-1113 (2006).
29. T. M. Muanza, A. P. Cotrim, M. McAuliffe, A. L. Sowers, B. J. Baum, J. A. Cook, F. Feldchtein, P. Amazeen, C. N. Coleman, and J. B. Mitchell, "Evaluation of radiation-induced oral mucositis by optical coherence tomography," *Clin. Cancer Res.* **11**, 5121-5127 (2005).
30. P. Wilder-Smith, M. J. Hammer-Wilson, J. Zhang, Q. Wang, K. Osann, Z. Chen, H. Wigdor, J. Schwartz, and J. Epstein "In vivo imaging of oral mucositis in an animal model using optical coherence tomography and optical Doppler tomography," *Clin. Cancer Res.* **13**, 2449-2454 (2007).
31. Y. Yasuno, V. D. Madjarova, S. Makita, M. Akiba, A. Morosawa, C. Chong, T. Sakai, K. P. Chan, M. Itoh, and T. Yatagai, "Three-dimension and high-speed swept-source optical coherence tomography for *in vivo* investigation of human anterior eye segments," *Optics Express* **13**, 10652-10664 (2005), <http://www.opticsexpress.org/abstract.cfm?uri=oe-13-26-10652>.
32. Y. Hori, Y. Yasuno, S. Sakai, M. Matsumoto, T. Sugawara, V. D. Madjarova, M. Yamanari, S. Makita, T. Yasui, T. Araki, M. Itoh, and T. Yatagai, "Automatic characterization and segmentation of human skin using three-dimensional optical coherence tomography," *Opt. Express* **14**, 1862-1877 (2006), <http://www.opticsinfobase.org/abstract.cfm?URI=oe-14-5-1862>.
33. S. A. Glantz, *Primer of Biostatistics* (McGraw-Hill Medical Pub., New York, 2005).

1. Introduction

Oral cancer is the fifth most common cancer in the world [1]. The worldwide annual incidence of oral cancers was estimated to be 274,000, accounting for 2.5% of all malignancies in both sexes in 2002 [2]. Oral cancer occurs with an annual incidence of approximately 29,370 cases in the United States [3]. In Taiwan, oral cancer is the fourth main cause of death in males and the sixth in both sexes among all cancers. The main etiologies that cause oral squamous cell carcinoma (SCC) in Taiwan are areca quid chewing, cigarette smoking, and alcohol consumption. Oral leukoplakia (OL), oral erythroleukoplakia (OEL), and oral verrucous hyperplasia are three common precancerous lesions that may transform into an SCC or a verrucous carcinoma. Oral mucosal lesions with benign epithelial hyperplasia (EH) and mild dysplasia are reversible lesions. They can return to healthy oral mucosa if patients stop their harmful oral habits. However, oral lesions with moderate dysplasia (MD) or severe dysplasia usually develop further into an SCC. The malignant transformation rates of oral premalignant lesions are reported to be 1-7% for homogenous thick OL, 4-15% for granular or verruciform OL, 18-47% (28% in average) for OEL, 4-11% for MD, and 20-35% for severe dysplasia [4].

Optical coherence Tomography (OCT) has attracted much attention for biomedical imaging because of its noninvasive, high-speed, and 3-D imaging nature [5, 6]. Recently, in the development of the Fourier-domain OCT technique, including spectral-domain OCT (SD-OCT) [7-10] and swept-source OCT (SS-OCT) [11, 12], the system sensitivity and imaging speed of such a system have been greatly improved when compared with those of the time-domain OCT technique [13-15]. In either SD-OCT or SS-OCT, the amplitude and echo time delay of the backscattered light are resolved through fast Fourier transform of the collected interfered spectral data. In SD-OCT, a high-speed spectrometer is used as the wavelength-resolved detection unit, which makes the mechanical scanning component in the reference arm unnecessary. On the other hand, in an SS-OCT system, the use of a frequency-swept laser source eliminates the requirement of the spectrometer for detection purpose. Therefore, an SS-OCT system has several advantages over those of an SD-OCT system, including high robustness in system setup, higher imaging speed, and higher sensitivity. High-speed SS-OCT operation with a polygon-mirror tuning filter in the spectral range of 1.3 μm has been implemented [11]. An SS-OCT system with the swept laser source near 1 μm in wavelength was also reported [16]. Such a system can reach a larger imaging depth, such as posterior eye, and is suitable for ophthalmic scanning in choroid study [17]. SS-OCT is particularly important for imaging in the wavelength ranges of 1 and 1.3 μm , in which charge-coupled devices (CCDs) or detector arrays are not well developed yet. Although a swept laser source may have the problem of intensity fluctuation in output spectrum, the use of balanced detection has made the system noise of SS-OCT tremendously reduced.

OCT has been widely used for oral cavity scanning. The images of human tooth and oral mucosa obtained by using a time-domain OCT system were first demonstrated in 1998 [18-20]. In 2004, *ex-vivo* OCT images of malignant mucosa of hamster cheek punches were acquired for studying the feasibility of using OCT scanning for oral disease diagnosis [21-23]. Later, *in-vivo* and 3-dimensional images of the same subject were also reported [24,25]. In clinical application of OCT to oral cancer diagnosis, *in-vivo* benign and malignant human oral mucosa images were compared [26]. Besides, OCT has been used for the study of laryngeal cancer [27,28] and the evaluation of radiation-induced oral mucositis [29,30]. In this paper, we report the analysis and statistics results of SS-OCT scan images in using three diagnosis indicators, including the standard deviation of an A-mode scan signal profile, the exponential decay constant of an A-mode-scan spatial-frequency spectrum, and the epithelium (EP) thickness when the boundary between EP and lamina propria (LP) can still be identified. Besides normal oral mucosa, three groups of buccal mucosa samples, including EH, MD, and SCC, are collected for analysis. Generally, in abnormal oral mucosal samples, the standard deviation becomes larger, the decay constant of the spatial-frequency spectrum becomes smaller, and the epithelium becomes thicker. The sensitivity and specificity of the three indicators are evaluated for different groups of oral mucosa samples (normal, EH, MD, and

SCC). In section 2 of this paper, the SS-OCT system and specifications are described. In section 3, the calibration procedures of SS-OCT images for the diagnosis indicators are presented. Then, in section 4, the statistics of the diagnosis indicators, including specificity and sensitivity, are discussed. Finally, the conclusions are drawn in section 5.

2. SS-OCT Scan

Figure 1 shows the layout of the portable SS-OCT system used in the hospital for clinical scanning. A sweeping-frequency laser source (Santec) with the output spectral sweeping full-width at half-maximum of 110 nm, centered at 1310 nm, is used as the light source. The light source can provide 6 mW in output power. Its sweep rate can reach 20 kHz. It is connected to a Mach-Zehnder interferometer consisting of two couplers and two circulators. A neutral density (ND) filter is used in the reference arm to maximize the system sensitivity. The interference fringe signal is detected by a balanced photodetector (PDB150C, Thorlabs) and sampled by a high-speed digitizer (PXI-5122, National Instrument). The interfered signal is rescaled by using the phase-oriented fringe analysis technique [31]. The system dispersion is compensated by a software compensation scheme [9]. The laser power incident onto the tissue sample is around 1.5 mW. The achieved SS-OCT system sensitivity and axial resolution in free space are 103 dB and 8 μm at the depth of 1 mm, respectively. In the sample arm, the lateral scanning is implemented with a handheld probe consisting of a linear stepping motor (Haydon), which is used to achieve a scanning speed of 10 cm/s and a 1-cm scanning length. In clinical application, the whole probe is wrapped by a plastic plate to protect the optical components inside the probe. After the scanning of a patient, the wrapped plastic plate is discarded and the whole probe is sterilized with 70 % ethanol. The lateral resolution of SS-OCT scanning is 15 μm . An SS-OCT image frame consisting of 2000 A-mode scans can be acquired within 0.1 s.

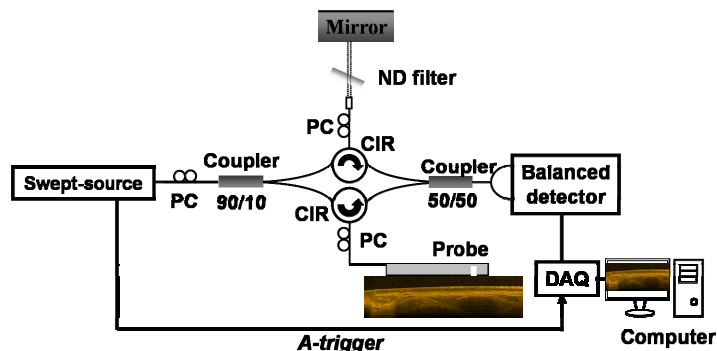


Fig. 1 SS-OCT setup used for clinical scanning. PC: polarization controller, CIR: circulator.

The SS-OCT system is used for clinical scan of 32 patients with age ranging from 30 through 77 years old. At each diagnosis, several SS-OCT 2-D scans are performed with the probe lightly contacting on the surface of representative portion of oral mucosal lesions. Also, healthy oral mucosal surface nearby is scanned for comparison. Then, biopsy specimen is taken from scanned portion of the oral lesion. Since it is difficult to match exactly the locations of biopsy and SS-OCT scan, we define a square of 5 mm in dimension as a basic unit of diagnosis. In other words, we use the biopsy and the SS-OCT scan results at a distance within 5 mm for comparison and hence the true or false decision based on SS-OCT scan. In analyzing OCT-scan images, home-made processing algorithm based on LabVIEW (National Instrument) is prepared. First, the signal of the plastic plate is removed from a B-mode scan image. Next, the surface of oral mucosa and the boundary between EP and LP layers are identified for evaluating the EP layer thickness. Then, the standard deviation of A-mode scan signal intensity in a range from 100 through 250 μm in depth for each A-mode scan is calculated. In the early stage of oral cancer, the tumor cell starts developing in the EP layer.

Therefore, the calculation of the standard deviation in the EP layer can help us in the diagnosis of oral precancer in the early stage. From the OCT scanning results of healthy volunteers, the EP thicknesses of healthy mucosa are always smaller than 300 μm . To avoid the strong scattering signals from the tissue surface and the basement membrane, the depth range from 100 through 250 μm was chosen for evaluating the standard deviation. Finally, after the Fourier transform of an A-mode scan profile covering the whole scan depth, the exponential-decay constant of the corresponding spatial-frequency spectrum is evaluated. Although our SS-OCT probe can reach almost every corner of the oral cavity of a patient, we will focus the discussions on the diagnosis results of lesions on bilateral buccal mucosae. In Taiwan, buccal SCCs are the most commonly diagnosed oral cancers.

3. Process of SS-OCT Images for the Indicators of Mucosa Diagnosis

Figure 2 shows the clinical photograph of a buccal SCC. The red and blue arrows indicate SS-OCT scan positions (1 cm in B-mode scan length) for the cancerous and normal oral mucosal tissues, respectively. Biopsy specimen is taken from the location of the red arrow. Figure 3(a) and (b) show the SS-OCT scanning images of the cancerous (a) and normal oral mucosal (b) portions indicated by the red and blue arrows, respectively, in Fig. 2. In the cancerous tissue, the boundary between EP and LP layers disappeared in the whole B-mode scan range. Here, the bright thin layers on tissue surfaces originate from the plastic plate (PP) used to cover the probe for preventing from contamination. The vertical red and blue lines and horizontal white arrows indicate the ranges of detailed analyses later. Figure 4(a) shows a histology image of normal mucosa to clearly demonstrate the EP and LP layers. Figure 4(b) shows the histological picture of the early invasive SCC illustrated in Figs. 2 and 3(a). Histologically, it shows hyperkeratosis and EH with MD and elongated epithelial ridges. Dysplastic cells breaking the basement membrane and invading into the LP are also found in other areas (not shown in Fig. 4(b)). The undulated arrangement of the epithelial ridges is well shown in the left one-third portion of Fig. 3(a). The connective tissue papillae (indicated by arrows) in Fig. 4(b) correspond to the almost vertical dark stripes in the left one-third portion of Fig. 3(a).

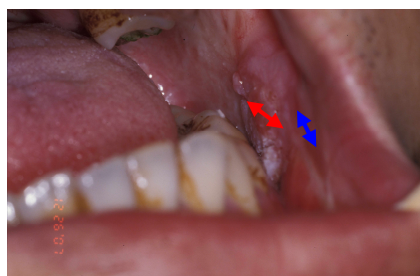


Fig. 2. Clinical photograph of a buccal squamous cell carcinoma. The red and blue arrows indicate SS-OCT scan positions for cancerous and normal oral mucosal tissues, respectively.

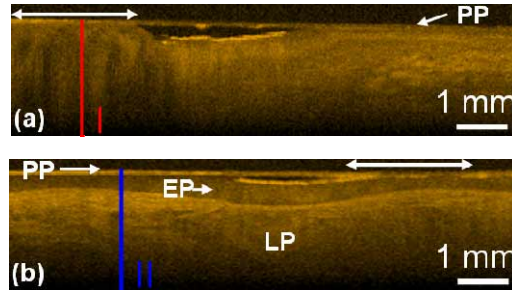


Fig. 3. SS-OCT scanning images of the cancerous (a) and normal oral mucosal (b) tissues indicated by the red and blue arrows, respectively, in Fig. 2. In the cancerous tissue, the boundary between EP and LP layers disappeared in the whole B-mode scan range. The red and blue vertical lines (labeled as I and II, respectively) and horizontal white arrows indicate the ranges of detailed analyses later. PP: plastic plate.

Figures 5(a) and (b) show the A-mode scan profiles of the red and blue vertical lines in Figs. 3(a) and (b), respectively, for cancerous and normal oral mucosal tissues. In the normal oral mucosa of Fig. 5(b), one can see sharp spikes between 400 and 500 μm in depth corresponding to the boundary between EP and LP layers. However, in the cancerous tissue of Fig. 5(a), such a clear boundary is not seen. The peak around 700 μm can be due to the residual boundary after EP layer became thickened in the early oral cancer evolution stage. An important feature in the comparison between Figs. 5(a) and (b) is the stronger signal intensity fluctuation in the cancerous tissue. The standard deviation, SD, of such fluctuations will be used as one of the diagnosis indicators with SS-OCT. In normal oral mucosa, the size and nuclear-to-plasma ratio of epithelial cells in EP is essentially quite uniform. The epithelial cells are closely arranged leading to a statistically homogenous distribution. However, in abnormal or cancerous mucosa, the tumor cells replace epithelial cells and tend to aggregate into a cluster structure called cancer nest. The size of cancer nest varies from place to place. Also, the cell size and nuclear-to-plasma ratio of tumor cell inside a cancer nest are non-uniform. The intra-cancer nest space is occupied by other cells or tissues, including inflammation cells, fibroblast, and connective tissues. Therefore, with such a more random distribution, the composition scale size of abnormal or cancerous oral mucosa in statistics becomes larger, when compared with that of normal oral mucosa. In this situation, it is expected that OCT scanning for acquiring the backscattering signal reflects the similar trend of statistical characteristics. Hence, in the spatial-frequency spectrum of an A-mode scan profile, the relative intensities of the low-spatial-frequency components in contrast to those of the high-spatial-frequency components in an abnormal sample are expected to be higher than those in a normal sample. Such a trend can be observed in Figs. 5(c) and (d), which are obtained by Fourier transforming the profiles in Figs. 5(a) and (b), respectively. To compare the relative intensities of the low-spatial-frequency components, we fit the first 50 data points of spatial frequency at the low-frequency end (including the DC component) with an exponential decay curve to obtain a decay constant, α . A smaller α corresponds to a spectrum of relatively stronger low-frequency components, as the case of the cancerous tissue. The exponential fitting represents a simple method for evaluating the trend of stronger low-frequency components in an abnormal sample. Searching for a possibly better method is one of the issues of further investigation. The choice of the first 50 data points is an optimized result, representing the optimized condition for the data we have collected so far. It can be modified when we collect more samples. The α values of the cancerous and normal oral mucosa are demonstrated in Figs. 5(c) and (d), respectively. Their difference is quite significant (0.0723 μm versus 0.0912 μm). The α value can be used as another diagnosis indicator with SS-OCT.

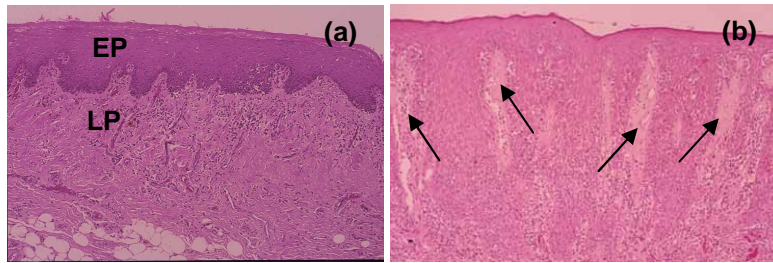


Fig. 4 (a) A histology image of normal mucosa. (b) Histological image of an early invasive squamous cell carcinoma in Figs. 2 and 3(a). The EP is hyperplastic with MD and elongated epithelial ridges. Dysplastic cells breaking the basement membrane and invading into the lamina propria are also found in other areas which are not shown here. The undulated arrangement of the epithelial ridges is well shown in the left one-third portion of Fig. 3(a). The connective tissue papillae (indicated by arrows) here correspond to the almost vertical dark stripes in the left one-third portion of Fig. 3(a).

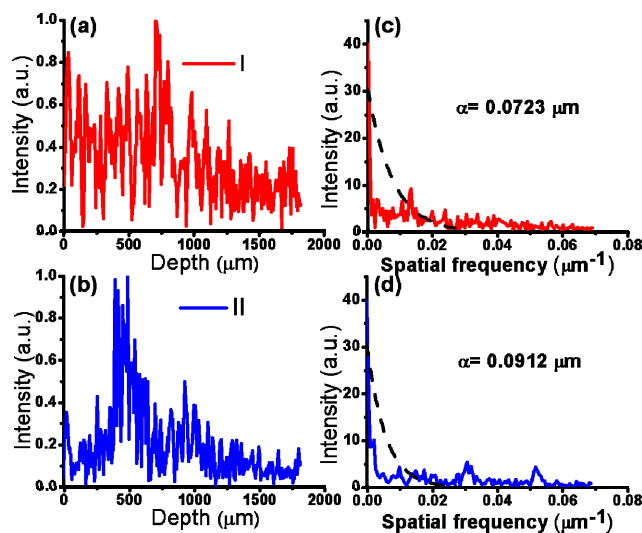


Fig. 5. Parts (a) and (b): A-mode scan profiles of the red and blue vertical lines in Figs. 3(a) and (b), respectively, for the cancerous and normal oral mucosa. Parts (c) and (d) are obtained by Fourier transforming the profiles in parts (a) and (b), respectively, to demonstrate the spatial-frequency spectra. The exponential decay constants, α , of the spectra are shown.

Figures 6(a) and (b) show the evaluated SD values as functions of lateral distance in the B-mode scans of the cancerous and normal oral mucosa tissues with the ranges indicated by the horizontal white arrows in Figs. 3(a) and (b), respectively. Although the SD value fluctuates along B-mode scan, its relative level in comparing Figs. 6(a) and (b) shows a significant difference between the cancerous and normal oral mucosa tissues. The mean value of SD over such a 2-mm lateral range will be used as a diagnosis indicator. The mean values of the cancerous and normal oral mucosa tissues are demonstrated in Figs. 6(a) and (b). A significant difference (0.21482 for the cancerous tissue versus 0.07708 for normal oral mucosa) can be seen. Similar results of α value are demonstrated in Fig. 7. Here, Figs. 7(a) and (b) show the evaluated α values as functions of lateral distance in B-mode scans of the cancerous and normal oral mucosa tissues with the ranges indicated by the horizontal white arrows in Figs. 3(a) and (b), respectively. Although the α value fluctuates along B-mode scan, its relative level in comparing Figs. 7(a) and (b) shows a significant difference between the cancerous and normal oral mucosa tissues. The mean of α value over such a 2-mm lateral

range will be used as another diagnosis indicator. The mean values of the cancerous and normal oral mucosa tissues are demonstrated in Figs. 7(a) and (b). A significant difference ($0.06926 \mu\text{m}$ for the cancerous tissue versus $0.08217 \mu\text{m}$ for normal oral mucosa, which represents a difference of 18.6 %) can be seen. We have also evaluated the standard deviations of the α values in Figs. 7(a) and (b) to give 0.00805 and $0.00979 \mu\text{m}$ for the cancerous and normal tissues, respectively. Here, one can see that the percentage standard deviations in the cases of cancerous and normal tissues are 12.8 and 11.9 %, respectively. However, the difference of the average values between the two cases is as large as 18.6 %.

In the early stage of oral cancer, the cancer cells start accumulating in the EP layer. In EH and precancer lesions, EP layer usually becomes thicker. The boundary between EP and LP layers eventually disappears if the cancerous condition continues to evolve. Therefore, before the boundary disappears, the EP thickness, which is defined as T , is another good indicator of diagnosis. To evaluate the thickness of the EP layer, a segmentation algorithm in LabVIEW was prepared [32]. First, along an A-mode scan profile, we can easily identify the image range of the plastic plate. After removing this portion of image, the location of the tissue surface can be obtained. Then, we search a local maximum along each A-mode scan profile below the tissue surface in a depth range of 1.5 mm for the depth of the basement membrane. If the difference between this depth and the corresponding value of the neighboring A-mode scan profile is smaller than a threshold value (10 % in our calculation), this depth is accepted as the boundary between the EP and LP layers; otherwise, two reasonable depths of basement membrane in the neighboring A-mode scan profiles on the two sides are averaged to give an acceptable depth for the EP and LP interface. Figure 8(a) shows an SS-OCT image of an EH lesion (identified by biopsy), in which the boundary between EP and LP layers can still be identified. Roughly speaking, the left one-half image shows normal oral mucosa. However, the right one-half clearly shows thickened EP layer. Figure 8(b) shows the variation of T along the B-mode scan in the whole lateral range of Fig. 8(a). One can see that the T value in the left one-half is always smaller than $300 \mu\text{m}$. Beyond 5 mm in the lateral distance, it increases up to 1.2 mm . This significant difference implies that the T value can be an effective indicator of diagnosis, particularly in the early stage of oral cancer development.

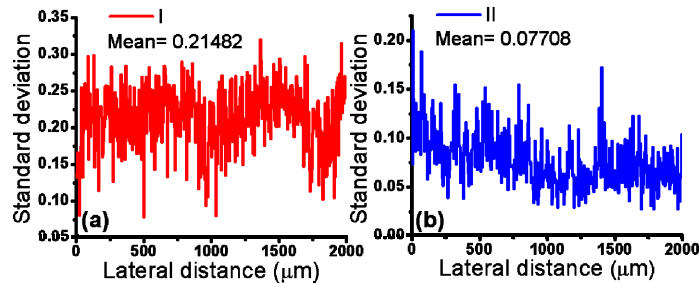


Fig. 6. Evaluated SD values as functions of lateral distance in the B-mode scans of the cancerous and normal oral mucosa with the ranges indicated by the horizontal white arrows in Figs. 3(a) and (b), respectively.

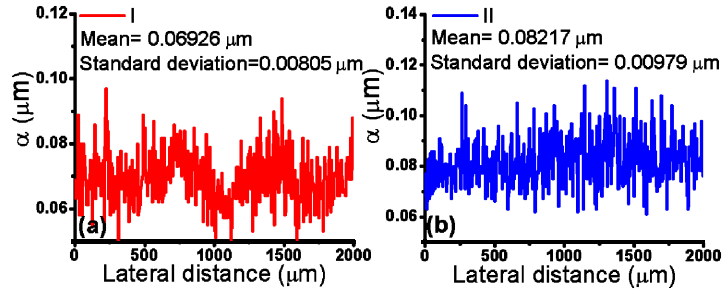


Fig. 7. Evaluated α values as functions of lateral distance in the B-mode scans of the cancerous and normal oral mucosa tissues with the ranges indicated by the horizontal white arrows in Figs. 3(a) and (b), respectively.

4. Sensitivity and Specificity

To understand the specificity and sensitivity of using the three above-mentioned diagnosis indicators including, SD, α , and T, we scan 16 EH, 18 MD and 15 SCC lesions from the buccal mucosa of 32 patients (including 31 male and one female) with an age range of 30-77 years old. All the male patients have the habit of areca quid chewing. Biopsy of the scanned site of each oral lesion is done after each SS-OCT scan to confirm the pathological diagnosis of the oral lesion. The adjacent oral mucosa covered with smooth, intact and healthy-looking oral mucosa is chosen for SS-OCT scan and used as normal controls. No biopsy is performed for the scanned normal oral mucosa. Histopathological diagnosis is made by microscopical examination of the biopsy specimens. The EH lesion shows an increase in epithelial thickness and surface parakeratosis or hyperkeratosis. No dysplastic epithelial cell is found in the EH lesion. MD is diagnosed when enough dysplastic cells are present in the basal two thirds but no more than the basal two-third of the oral EP. An SCC lesion shows invasion of nests of cancer cells into the underlying connective tissue.

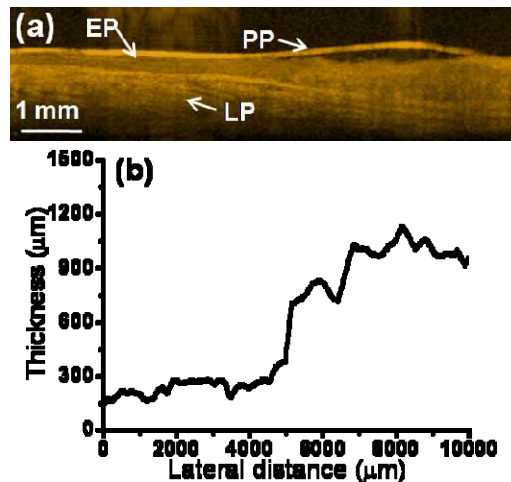


Fig. 8. (a) An SS-OCT scan image of an EH lesion, in which the boundary between EP and LP layers can still be identified. (b) Evaluated EP layer thickness, T, as a function of lateral distance in the B-mode scan.

In each SS-OCT scan, a 2-mm B-mode scan range is used for evaluating the mean values of SD, α , and T. From the 32 patients, a total of 84 samples including 35 normal control samples (T values can be evaluated from all 35 samples), 16 EH samples (T values can be evaluated from all 16 samples), 18 MD samples (T values can be evaluated only from 12

samples), and 15 SCC samples (no T value can be evaluated from any sample) are collected. SD and α data are evaluated from these 84 samples. The data sets are used for evaluating the specificity and sensitivity of the diagnosis indicators. Figure 9 shows the SD data point distributions of the four groups of sample, including EH (circles), MD (diamonds), SCC (triangles), and normal control mucosa (squares). Here, the significantly larger SD values for the MD and SCC groups, compared with those of the other two groups, can be clearly seen, indicating that SD is a good diagnosis indicator. In Table 1, we show the specificity and sensitivity of using SD as a diagnosis indicator with various criteria from 0.085 to 0.16. The specificity is defined as the percentage of normal control samples, in which SDs of SS-OCT scans are smaller than or equal to the specified SD level (judged to be normal based on SS-OCT scan results). Although EH is an abnormal condition, it is a benign and reversible lesion and deserves the understanding of its microstructure with SS-OCT scanning. Therefore, we evaluate two specificity values in the two conditions of including and excluding the EH samples for evaluation. Based on 51 samples (35 normal control and 16 EH samples), the specificity increases from 45.1 to 100 % when the specified SD level increases from 0.085 to 0.16. Based on 35 normal control samples only (excluding EH samples), the specificity increases from 60 to 100 % when the specified SD level increases in the same range. Here, one can see that the specificity is higher if the EH samples are regarded as abnormal. The sensitivity is defined as the percentage of abnormal samples, in which SDs in SS-OCT scans are larger than the specified SD level (judged to be abnormal based on SS-OCT scan results). Here, we also consider the two conditions of including and excluding EH samples in evaluating the sensitivity. Based on the 49 abnormal samples (16 EH, 18 MD and 15 SCC samples), the sensitivity decreases from 97.96 to 63.27 % when the specified SD level increases from 0.085 to 0.16. Based on the 33 abnormal samples (18 MD and 15 SCC samples), the sensitivity decreases from 100 to 87.88 % when the specified SD level increases from 0.085 to 0.16. Therefore, the sensitivity is higher if the EH samples are regarded as “normal”. Based on the statistics of the collected data, the choice of SD value of 0.12 can result in 100 % for both specificity and sensitivity if EH is excluded in evaluation. To further understand the effectiveness of using SD as diagnosis indicator for differentiating different oral mucosa lesions, in Table 2, we list the sensitivity of different oral mucosal sample groups. Because EH is a stage between normal oral mucosa and precancerous lesions which include moderate and severe dysplasia, we evaluate both specificity and sensitivity for the EH group. Here, one can see that SD is an effective indicator for diagnosing MD and SCC, but not EH.

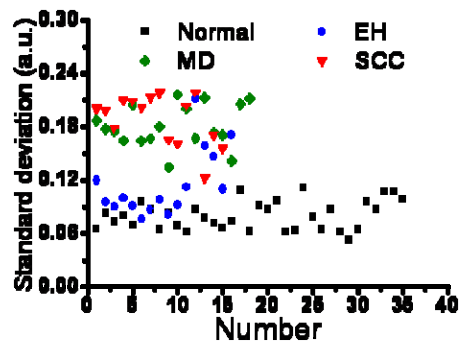


Fig. 9. SD data point distributions of the four groups of data.

Table 1. Specificity (%) and sensitivity (%) of using SD as a diagnosis indicator with various criteria from 0.085 to 0.16. N: number of sample. The labels of a-i for the SD values will be used for assigning the data points in Fig. 12.

	N	SD								
		0.085 ^a	0.09 ^b	0.1 ^c	0.11 ^d	0.12 ^e	0.13 ^f	0.14 ^g	0.15 ^h	0.16 ⁱ
Specificity (including EH)	51	45.1	56.9	76.5	84.3	90.2	92.2	92.2	98	100
Specificity (excluding EH)	35	60	74.3	88.6	97.1	100	100	100	100	100
Sensitivity (including EH)	49	98	93.9	83.7	81.6	77.6	73.5	71.4	67.4	63.3
Sensitivity (excluding EH)	33	100	100	100	100	100	97	93.9	90.9	87.9

Table 2. Specificity (%) and sensitivity (%) of using SD as a diagnosis indicator for different groups of abnormal oral mucosal samples. N: number of sample.

Sample group	N	SD									
		0.085	0.09	0.1	0.11	0.12	0.13	0.14	0.15	0.16	0.17
Specificity of EH	16	12.5	18.8	50	56.3	68.8	75	75	81.3	87.5	87.5
Sensitivity of EH	16	87.5	81.3	50	43.8	31.3	25	25	18.8	12.5	12.5
Sensitivity of MD	18	100	100	100	100	100	100	94.4	88.9	88.9	66.7
Sensitivity of SCC	15	100	100	100	100	100	100	100	100	93.3	80

Figure 10 shows the α data point distributions of the four groups of data, similar to Fig. 9 for SD. Here, again one can see the clear difference between the groups of normal control and abnormal oral mucosal lesions even though the difference is smaller in comparing with that of SD. In Table 3, we show the specificity and sensitivity of using α as a diagnosis indicator with various criteria from 0.074 to 0.08 μm . The specificity is defined as the percentage of normal control samples, in which α values in SS-OCT scans are larger than or equal to the specified α level (judged to be normal based on SS-OCT scan results). Similar to Table 1, in Table 3, we consider the two conditions of including and excluding the EH samples for evaluating the specificity and sensitivity. When 16 EH samples are evaluated together with 35 normal control samples, the specificity decreases from 92.16 to 62.75 % as the specified α value increases from 0.074 to 0.08 μm . When considering the 35 normal control samples only, the specificity decreases from 100 to 74.29 % as the specified α value increases from 0.074 to 0.08 μm . The sensitivity is defined as the percentage of abnormal oral mucosal samples, in which α values in SS-OCT scans are smaller than the specified α level (judged to be abnormal based on SS-OCT scan results). When EH, MD and SCC samples are considered together, the sensitivity increases from 40.82 to 83.67 % as the specified α value increases from 0.074 to 0.08 μm . When only 18 MD and 15 SCC samples are evaluated together, the sensitivity increases from 45.45 to 93.94 % as the specified α value increases from 0.074 to 0.08 μm . From the statistics of the collected data, the choice of α value between 0.078 and 0.079 μm can be regarded as the optimum condition if the EH samples can be excluded in statistics. To further understand the effectiveness of using α as a diagnosis indicator for differentiating different oral mucosa lesions, in Table 4, we list the specificity and sensitivity of different sample groups. Here, one can see that the α value is also an effective indicator for diagnosing MD and SCC, but not EH.

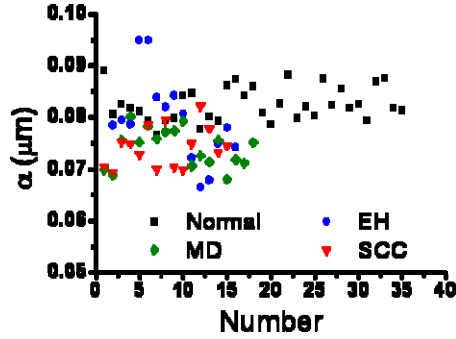


Fig. 10. Decay constant, α , data point distributions of the four groups of data.

Table 3. Specificity (%) and sensitivity (%) of using the decay constant, α , as a diagnosis indicator with various criteria from 0.074 to 0.08 μm . N: number of sample. The labels of a-g for the α values will be used for assigning the data points in Fig. 12.

	N	α (μm)						
		0.08 ^a	0.079 ^b	0.078 ^c	0.077 ^d	0.076 ^e	0.075 ^f	0.074 ^g
Specificity (including EH)	51	62.8	76.5	84.3	86.3	88.2	88.2	92.2
Specificity (excluding EH)	35	74.3	91.4	94.3	97.1	100	100	100
Sensitivity (including EH)	49	83.7	77.6	67.4	61.2	61.2	47	40.8
Sensitivity (excluding EH)	33	93.9	87.9	81.8	72.7	72.7	51.5	45.5

Table 4. Specificity (%) and sensitivity (%) of using the decay constant, α , as a diagnosis indicator for different groups of abnormal oral mucosal samples. N: number of sample.

Abnormality condition	N	α (μm)						
		0.08	0.079	0.078	0.077	0.076	0.075	0.074
Specificity of EH	16	37.5	43.8	62.5	62.5	62.5	62.5	62.5
Sensitivity of EH	16	62.5	56.3	37.5	37.5	37.5	37.5	37.5
Sensitivity of MD	18	94.4	88.9	83.3	72.2	72.2	44.4	44.4
Sensitivity of SCC	15	93.3	86.7	80	73.3	73.3	60	46.7

Next, we evaluate the statistics of using EP thickness, T, as a diagnosis indicator. For this purpose, we can use only part of the collected SS-OCT scan samples, in which the boundary between EP and LP layers can still be identified. In total, 35 normal control, 16 EH, and 12 MD samples are used for evaluating the specificity and sensitivity, as shown in Fig. 11 and Table 5. The EP/LP boundaries disappear in all SCC samples. In Fig. 11, one can see that the T values of EH and MD samples are generally larger than those of normal control samples. In Table 5, we show the specificity and sensitivity of using T as a diagnosis indicator with various criteria from 150 to 600 μm , covering the two conditions of including and excluding EH samples. The specificity is defined as the percentage of normal samples, in which T values in SS-OCT scans are smaller than the specified T level (judged to be normal based on SS-OCT scan results). Based on the 35 normal control and 16 EH samples, the specificity increases from 3.92 to 86.27 % when the specified T level increases from 150 to 600 μm . Based on the 35 normal control samples only, the specificity increases from 5.71 to 100 % when the specified T level increases in the same range. The sensitivity is defined as the percentage of abnormal oral mucosal samples, in which T values in SS-OCT scans are larger

than the specified T level (judged to be abnormal based on SS-OCT scan results). Based on the 16 EH and 12 MD samples, the sensitivity decreases from 100 to 28.57 % when the specified T level increases from 150 to 600 μm . Based on the 12 MD samples only, the sensitivity decreases from 100 to 16.67 % when the specified T level increases in the same range. From the statistics of the collected data, the choice of T value of 300 μm can result in 82.86 % for specificity and in 92.86 % for sensitivity if the EH lesion is regarded as abnormal. In Table 6, we list the specificity and sensitivity of different sample groups. Here, one can see that T is an effective indicator for diagnosing EH and MD lesions. Figure 12 shows the receiver-operating characteristic curves of the three indicators under the condition of excluding the EH samples. The plots of the sensitivity values versus the values of one minus the specificity are always distributed in the upper-left corner (with respect to the dashed diagonal line), indicating the effectiveness of using the three indicators for oral cancer diagnosis based on the OCT technique. In Fig. 12, the letters next to the data points label the conditions shown in Tables 1, 3, and 5. It is noted that the p values of all the three proposed indicators under the condition of excluding the EH samples were evaluated to give values always smaller than 0.001, which is much smaller than the threshold value of 0.05 for reliable statistical analysis [33].

The statistics shown in Tables 1-6 were obtained by using the universal criteria of SD, α , and T. However, because the microstructures of oral mucosa may significantly vary among people and even among different locations in the oral cavity of an individual, a universal criterion for diagnosing a disease may lead to inaccurate results. In the following, we present the statistics of using the SS-OCT scan result in normal mucosa of an individual patient as the reference of the nearby abnormal mucosa for building the diagnosis criteria. As mentioned before, for each patient, we always scan normal control mucosa near an abnormal oral lesion. With the available normal control mucosa data, we can use their SD, α , and T values as the references for designing the criteria of diagnosis. For instance, we can use a certain percentage of the normal control SD, α , or T value as the criterion. Based on this reference, we can eliminate the factor of tissue structure variation among different patients. Table 7 shows the specificity and sensitivity of using 100 to 150 % the normal control SD value (relative SD) of each individual patient as the criteria. Among the three groups of abnormal oral mucosal samples, the relative SD is an effective indicator for MD and SCC, but not for EH. This conclusion is the same as that of the universal criteria (see Table 2). Table 8 shows the specificity and sensitivity of using 90 to 105 % the normal control α value (relative α) of each individual patient as the criteria. Except for MD, the α value does not seem to be a good diagnosis indicator. Table 9 shows the specificity and sensitivity of using 100 to 150 % the normal control T value (relative T) of each individual patient as the criteria. Similar to the case of universal criterion, T value is quite a good indicator for EH and MD lesions. Generally speaking, the specificity and sensitivity of using the relative criteria are similar to those of using the universal criteria. However, since in clinical practice we always perform a few normal control SS-OCT scans near an abnormal oral mucosal lesions under examination, it is more practical to use the relative criteria in diagnosing the abnormal oral mucosal lesions.

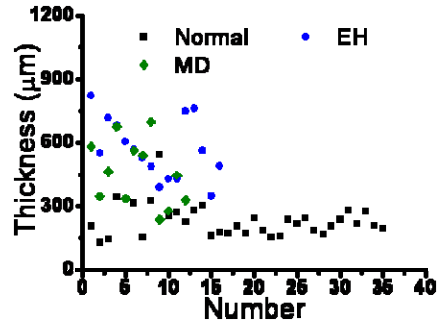


Fig. 11 T data point distributions of the three groups of data.

Table 5. Specificity (%) and sensitivity (%) of using the epithelium thickness, T, as a diagnosis indicator with various criteria from 150 to 600 μm . N: number of sample. The labels of a-i for the T values will be used for assigning the data points in Fig. 12.

	N	T (μm)									
		150 ^a	200 ^b	250 ^c	300 ^d	350 ^e	400 ^f	450 ^g	500 ^h	550 ⁱ	600
Specificity (including EH)	51	3.9	25.5	47.1	56.9	68.6	70.6	74.5	78.4	82.4	86.3
Specificity (excluding EH)	35	5.7	37.1	68.6	82.9	97.1	97.1	97.1	97.1	100	100
Sensitivity (including EH)	28	100	100	96.4	92.9	78.6	75	64.3	53.6	46.4	28.6
Sensitivity (excluding EH)	12	100	100	91.7	83.3	58.3	58.3	50	41.7	33.3	16.7

Table 6. Specificity (%) and sensitivity (%) of using the epithelium thickness, T, as a diagnosis indicator for different groups of abnormal oral mucosal samples. N: number of sample.

Sample group	N	T (μm)									
		150	200	250	300	350	400	450	500	550	600
Specificity of EH	16	0	0	0	0	6.3	12.5	25	43.8	43.8	62.5
Sensitivity of EH	16	100	100	100	100	93.8	87.5	75	56.3	56.3	37.5
Sensitivity of MD	12	100	100	91.7	83.3	58.3	58.3	50	41.7	33.3	16.7

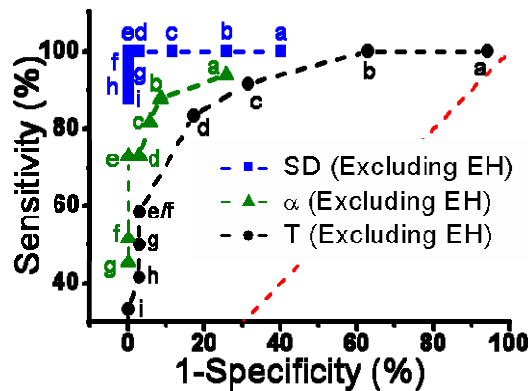


Fig. 12. Receiver-operating characteristic curves of the three indicators. The letters next to the data points label the conditions shown in Tables 1, 3, and 5.

5. Conclusions

We have used an SS-OCT system of 8 μm in free-space axial resolution, 103 dB in system sensitivity, and 20 kHz in A-mode scanning rate to clinically scan oral precancers and cancers. The statistics of using three diagnosis indicators, including the standard deviation of an A-mode scan signal profile, the exponential decay constant of an A-mode-scan spatial-frequency spectrum, and the epithelium thickness when the boundary between epithelium and lamina propria could still be identified, were evaluated. Besides normal control mucosa, three groups of abnormal buccal mucosa samples, including EH, MD, and SCC, were identified for analysis based on the histopathological examination of biopsy specimens. Generally, in abnormal oral mucosal lesions, the standard deviation became larger, the decay constant of the spatial-frequency spectrum became smaller, and the epithelium became thicker. The sensitivity and specificity of the three diagnosis indicators were calculated based on the universal and relative criteria of the three indicators. It was found that the SD and α are good diagnosis indicators for MD and SCC lesions. T is a good diagnosis indicator for EH and MD lesions. Although the results based on the universal and relative criteria were similar, it is more practical to use the relative criteria in diagnosing abnormal oral mucosal lesions.

Table 7. Specificity and sensitivity (%) of using the relative SD as a diagnosis indicator for different groups of abnormal oral mucosal sample based on the normal control conditions of individual patients. N: sample number.

Sample group	N	Relative SD (%)					
		100	110	120	130	140	150
Specificity of EH	16	31.3	31.3	50	62.5	68.8	75
Sensitivity of EH	16	68.8	68.8	50	37.5	31.3	25
Sensitivity of MD	18	100	100	100	100	100	100
Sensitivity of SCC	15	100	100	100	100	100	86.7

Table 8. Specificity and sensitivity (%) of using the relative α as a diagnosis indicator for different groups of abnormal oral mucosal samples based on the normal control conditions of individual patients. N: number of sample.

Sample group	N	Relative α (%)			
		105	100	95	90
Specificity of EH	16	12.5	31.3	43.8	81.3
Sensitivity of EH	16	87.5	68.8	56.3	18.8
Sensitivity of MD	18	100	100	61.1	50
Sensitivity of SCC	15	100	86.7	73.3	46.7

Table 9. Specificity and sensitivity (%) of using the relative T as a diagnosis indicator for different groups of abnormal oral mucosal samples based on the normal control conditions of individual patients. N: number of sample.

Sample group	N	Relative T (%)					
		100	110	120	130	140	150
Specificity of EH	16	0	0	0	6.3	18.8	25
Sensitivity of EH	16	100	100	100	93.8	81.3	75
Sensitivity of MD	12	100	100	100	91.7	91.7	83.3

Acknowledgement

This research was supported by National Health Research Institute, The Republic of China, under the grant of NHRI- EX97-9616EI.